UNIVERSITY OF CALIFORNIA SAN DIEGO

A Neural Network Model of Cancer Identifies Chemotherapies Synergistic with Autophagy Inhibition

A thesis submitted in partial satisfaction of the requirements for the degree Master of Science

in

Biology

by

Likitha Yadav Aradhyula

Committee in Charge:

Professor Trey Ideker, Chair
Professor Amy Kiger, Co-Chair
Professor Gen-Sheng Feng

2022

The thesis of Likitha Yadav Aradhyula is approved, and it is acceptable in quality and form for publication on microfilm and electronically.

University of California San Diego

2022

TABLE OF CONTENTS

LIST OF SUPPLEMENTAL FILES

aradhyula_single_drug_plate_maps.pdf

aradhyula_single_drug_atg_ratios.zip

aradhyula_single_drug_cell_count.zip

aradhyula_drug_combo_plate_maps.pdf

aradhyula_drug_combo_atg_ratios.zip

aradhyula_drug_combo_cell_count.zip

LIST OF FIGURES

LIST OF TABLES

ACKNOWLEDGEMENTS

I would like to acknowledge Dr. Trey Ideker for providing me the resources and means to pursue research the past four years. His immense support as the chair of my committee and as my PI pushed me to be the best researcher I can be.

This thesis, in full, is a reprint of the material as it will appear in A Neural Network Model of Cancer Identifies Chemotherapies Synergistic with Autophagy Inhibition. Aradhyula, Likitha Y; Silva, Erica; Fong, Samson H.; Rajaee, Lily; Ideker, Trey. The thesis author was the primary investigator and author of this paper.

ABSTRACT OF THE THESIS

A Neural Network Model of Cancer Identifies Chemotherapies Synergistic with Autophagy Inhibition

by

Likitha Yadav Aradhyula

Master of Science in Biology

University of California San Diego, 2022

Professor Trey Ideker, Chair
Professor Amy Kiger, Co-Chair

In cancer, autophagy has been shown to promote resistance to chemotherapy by inducing pro-survival mechanisms. This observation has led to basic and clinical studies combining chloroquine, an autophagy inhibitor, with standard chemotherapies. However, the range of particular chemotherapies likely to benefit from this combination remains unclear. Here we apply DrugCell, a deep learning model of the molecular pathways that govern cancer therapeutic response, to systematically prioritize drugs that promote cell survival through the

activation of autophagy. Using this approach, we analyze the response of tumor cell lines to 684 drugs, identifying 21 for which resistance or sensitivity is modulated by genetic mutations in autophagy pathways. We systematically screen these prioritized drugs against a fluorescent readout of autophagic flux, confirming that 14 stimulate this pathway and 1 leads to pathway suppression, for a hit rate of 15/22 or 71%. In contrast, only 1 in 6 of a control set of drugs is found to affect autophagy activity. Finally, we test eight of the autophagy activators for synergy with chloroquine treatment, finding that four are highly synergistic, producing a BLISS score greater than 10. These results suggest that, for these drugs (JQ1, tosedostat, leptomycin B, vorinostat), chloroquine inhibition of autophagic flux interferes with autophagy as a survival response.

Introduction

Autophagy is a highly conserved and tightly controlled set of processes by which eukaryotic cells sequester and deliver intracellular components to lysosomes for degradation. Autophagic flux ranges from basal levels that maintain cellular homeostasis to higher levels that aid in cellular adaptation to stresses, such as nutrient deprivation or bacterial infection (Levine & Kroemer, 2008, 2019).

Recent evidence indicates that autophagy promotes resistance of cancer cells to chemotherapy, through complex mechanisms that are still incompletely understood but appear to be context-specific (Sui et al., 2013, Paillas et al., 2012, Duan et al., 2011). Given the role autophagy plays in chemoresistance, basic and clinical studies have tested the combined use of chemotherapies along with the autophagy inhibitor chloroquine. For example, a study looked specifically at the combinatorial treatment of the pan erbB inhibitor PD168393 with the autophagy inhibitor chloroquine for malignant peripheral nerve sheath tumors (MPNSTs). They did observe increased cytotoxicity and caspase activation in the MPNSTs that were treated with PD168393 and chloroquine (Kohli et al., 2012). However, it is unclear whether multiple chemotherapies that treat MPNSTs would have the same effect when paired with chloroquine or if PD168393 and chloroquine would induce the same level of cytotoxicity in other tumor types.

Previous large-scale screens to identify autophagy activators have had a low hit rate, indicating such agents are rare (Balgi et al., 2009; Chauhan et al., 2015; Hundeshagen et al., 2011; Kaizuka et al., 2016; Zhang et al., 2007). Specifically, in one screen of about a thousand molecules, approximately 5% were identified as autophagy modulators (Kaizuka et al., 2016).

To increase the chances of identifying cancer drugs that activate autophagy, we took advantage of DrugCell, an interpretable deep learning model of chemotherapeutic response. It contains two input features: the genotypes of the cells, and the chemical structures of the drugs.

DrugCell organizes the genetic alterations of a cell by restricting connections among genes to those in the same pathway. These pathways are then hierarchically organized to reflect how a cell is organized. This structure, called visible neural network, allows DrugCell to infer the biological mechanisms that underlie cellular response to a specific treatment (Kuenzi et al., 2020).

Here, we report the results of a pipeline to selectively identify cancer therapies that should be paired with chloroquine. We first selected drugs by using DrugCell to prioritize therapies that are informative of autophagy mechanisms, indicating they are likely to modulate autophagy in cells, and found 71% of the drugs modulated autophagy. A subsection of these activators were screened again and determined 50% to be synergistic with chloroquine. These results suggest that, for these drugs, chloroquine-mediated inhibition of autophagic flux prevents the cell from using autophagy as a survival mechanism.

Results

Identifying Drugs that Interact with Mutations in Autophagy Pathways

We consulted DrugCell to prioritize drugs that are likely to be synergistic with chloroquine. As cell genotypes are integrated through a 'visible' neural network', the model can be interpreted to identify which components of the model are informative and responsible for the range of predictions for a specific drug (Figure 1A). Relative local increase in predictive performance (RLIPP) is the ratio between the performance of the parent model divided by the child model, which was used to score how likely the drugs modulate a specific pathway, in this case, autophagy. A RLIPP score greater than 1 indicates that the model learned additional information at the subsystem level. A RLIPP score less than 1 indicates that the model did not learn additional information at the subsystem level. With the drugs that had a RLIPP>1 for the autophagy pathway,

we performed a literature review to condense the list. We included drugs that were from different classes while having some in the same class to compare autophagy activity across the classes. Figure 1B shows the final candidate list of drugs we selected to test. To ensure DrugCell generated a candidate list of drugs that interact with autophagy, we selected six drugs (doxorubicin, trametinib, palbociclib, MK-2006, vinorelbine, olaparib) that had a low RLIPP score for the autophagy pathway, indicating these drugs are predicted to not modulate autophagy. These six drugs acted as negative controls and were tested in combination with our candidate drug list.

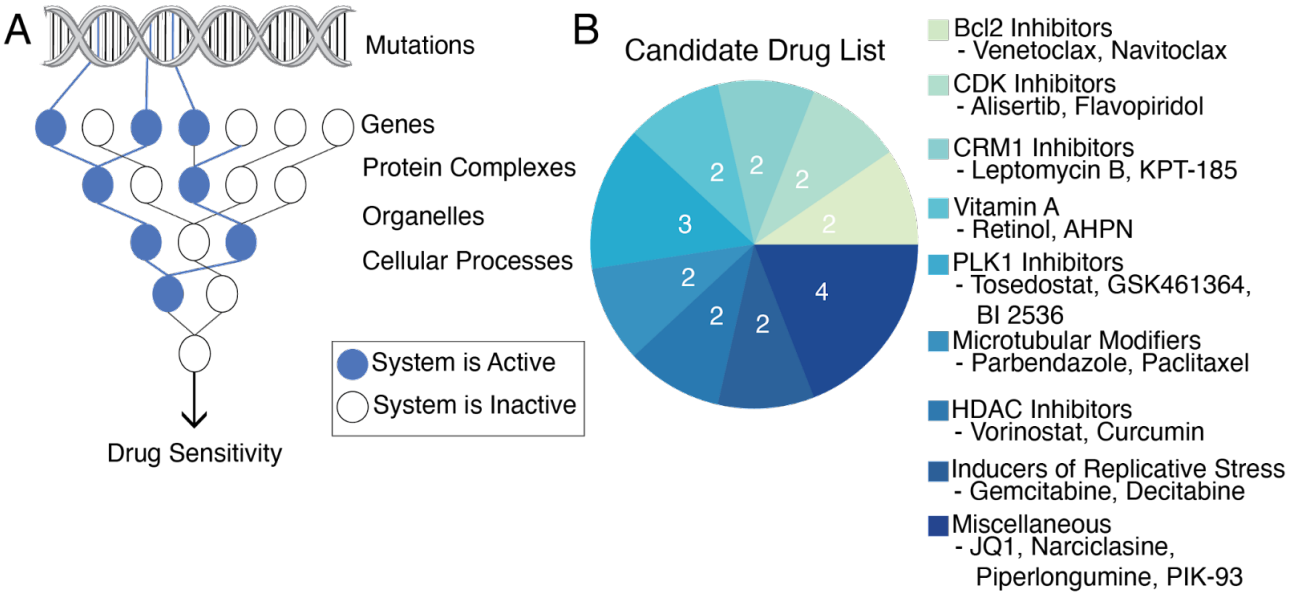

Figure 1. Candidate Drug List Derived from DrugCell

(A) Simplified overview of the visible neural network by which genotypes are embedded in DrugCell. Blue versus white nodes represent specific systems that are active versus inactive when predicting autophagy-modulating drugs.

(B) Pie chart showing classes of drugs for which the gene mutations within the autophagy subsystem are informative for drug response prediction.

Generation of Stable Single Clone Cell Lines that Measure Autophagic Flux

With the ultimate goal of generating a cell line that can accurately measure autophagic flux in drug screens, we utilized a fluorescent autophagy reporter (Kaizuka et al. 2016). The fluorescent reporter pMRX contains a functional GFP-LC3 domain and a nonfunctional RFP-LC3ΔG domain. When the reporter is expressed in cells, ATG4 cleaves the two domains, allowing the functional GFP-LC3 domain to be recruited to the autophagosome, where it gets degraded when autophagy is activated. As the LC3ΔG domain in RFP-LC3ΔG is nonfunctional, it remains in the cytoplasm as an internal control (Figure 2A). Hence, the ratio between the GFP and RFP fluorescence can be used to measure autophagy activity: High GFP/RFP ratio means less autophagy activity, and low GFP/RFP ratio means high autophagy activity.

We next worked to generate stable single clonal hTERT-RPE1 lines that express the pMRX reporter. To functionally validate the pMRX reporter in the cell lines, the RPE1-pMRX cell lines were subjected to two treatments: serum starvation alone and serum starvation with 5uM chloroquine (Figure 2B). As serum starvation induces autophagy, the GFP-LC3 in pMRX would get degraded by the autophagosome, whereas chloroquine blocks autophagy, preventing the degradation of GFP-LC3. As expected, the microscopy images under serum starvation alone showed decreased GFP fluorescence, and the images under serum starvation and 5uM chloroquine showed increased GFP fluorescence (Figure 2C). For all subsequent drug screens, we utilized two of the functionally validated single clonal RPE1-pMRX cell lines to ensure the results are accurate and not artifacts of the single clone cell line.

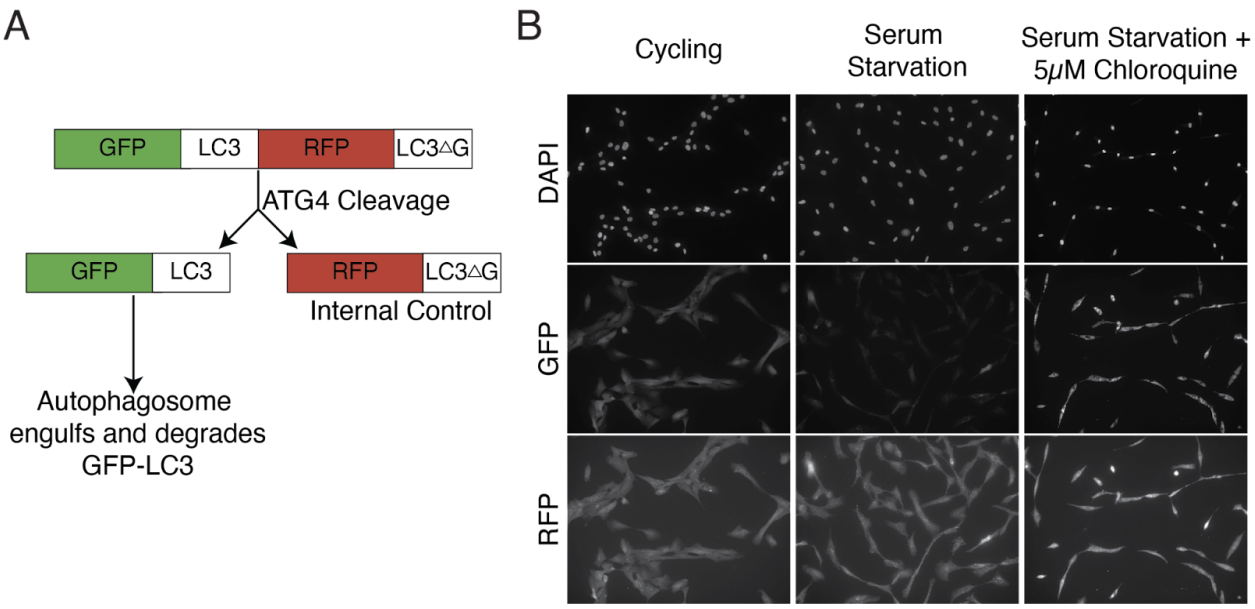

Figure 2. Generation of Stable Single Clone Cell Lines that Express pMRX

(A) Mechanism of pMRX reporter measuring autophagic flux

(B) Example diagram depicting expected GFP/RFP ratios dependent on level of autophagy activity

(C) Example of functionally validated single clone RPE1-pMRX under fluorescence microscopy: no treatment (Cycling), serum starvation (SS), and serum starvation with 5uM chloroquine (Chq) treatment. As expected, we observed a decrease in GFP/RFP (increase in autophagic flux) in cells under SS treatment and an increase in GFP/RFP (decrease in autophagic flux) in cells under SS + 5uM Chq treatment.

Dose-Dependent Response of Candidate Drug List on Autophagy

We next sought to determine which of the candidate chemotherapies do indeed modulate autophagy. For this purpose the RPE1-pMRX single clones were treated with each drug, at doses ranging from 0 to 50uM for 48 hours to measure the dose-dependent response of the chemotherapies on autophagy activity. We observed a decrease in GFP fluorescence when

RPE1-pMRX was treated with 5uM vorinostat (Figure 3A). As doses of vorinostat increased, there was a significant decrease in GFP/RFP ratio, indicating that vorinostat activates autophagy (Figure 3B). An increase in GFP fluorescence and GFP/RFP ratio was observed when RPE1-pMRX was treated with 0.89uM to 2.81uM navitoclax, which means that navitoclax inhibits autophagy (Figure 3A,C). Flavopiridol caused no change in GFP fluorescence and GFP/RFP ratio, indicating that flavopiridol is not a modulator of autophagy (Figure 3A,D). Out of the 21 candidate drugs tested, we found that 15 drugs caused a significant difference in GFP/RFP ratio in at least 20% of doses (p-value < 0.001, Figure 3E, S1). Of these, 14 drugs were found to be activators and 1, navitoclax, was found to be an inhibitor (Figure 3E). Out of the six drugs predicted by DrugCell to not be an autophagy modulator, only one, doxorubicin, was found to modulate autophagy (Figure 3E, S2). Moreover, the candidate drug list had a substantially greater number of doses for which a significant difference was found in GFP/RFP ratio compared to negative control drugs, indicating that DrugCell effectively prioritized drugs that modulate autophagy (15/21 (71%) versus 1/6 (17%); Figure 3F). We found that DrugCell is 12.5 times more likely to select an autophagy modulator rather than random selection, highlighting the effectiveness of DrugCell to select drugs that modulate a specific pathway.

We found that all of the replicative stress inducers, PLK1 inhibitors, and microtubular modifiers activated autophagy. For example, gemcitabine and decitabine are replicative stress inducers both of which had similar dose-dependent responses in viability and GFP/RFP ratio. Such within-class similarity was also seen in the microtubular modifiers tested (Figure S2). Such evidence suggests that modulators selected by DrugCell are clustered in a handful of mechanisms of action.

Figure 3. Effects of drug combinations on autophagic flux

(A) 10x microscopy images of RPE1-pMRX treated with no drug, 5uM vorinostat, 2.81uM navitoclax, or 0.05uM flavopiridol.

Figure 3. Effects of drug combinations on autophagic flux (Continued)

(B-D) Graphs of GFP/RFP ratios of RPE1-pMRX treated with a range of doses of vorinostat (B), navitoclax (C), or flavopiridol (D); statistical significance (p-value < 0.001) indicated by asterisks (**).

(E) Barplot of percent doses of each drug tested that had a p-value <0.001. Gray line at 20% represents the threshold drugs had to meet to be considered a modulator. Drugs that are in bold are the candidate drugs that DrugCell predicted to be autophagy modulators. Drugs that are not in bold are the drugs that DrugCell predicted to not be in autophagy modulators. Red means activator, green means inhibitor, and gray means non-modulator.

(F) Boxplot of the fraction of doses between the candidate drug list and negative control drugs that had significantly different GFP/RFP ratios; p-value calculated using the Matt Whitney test.

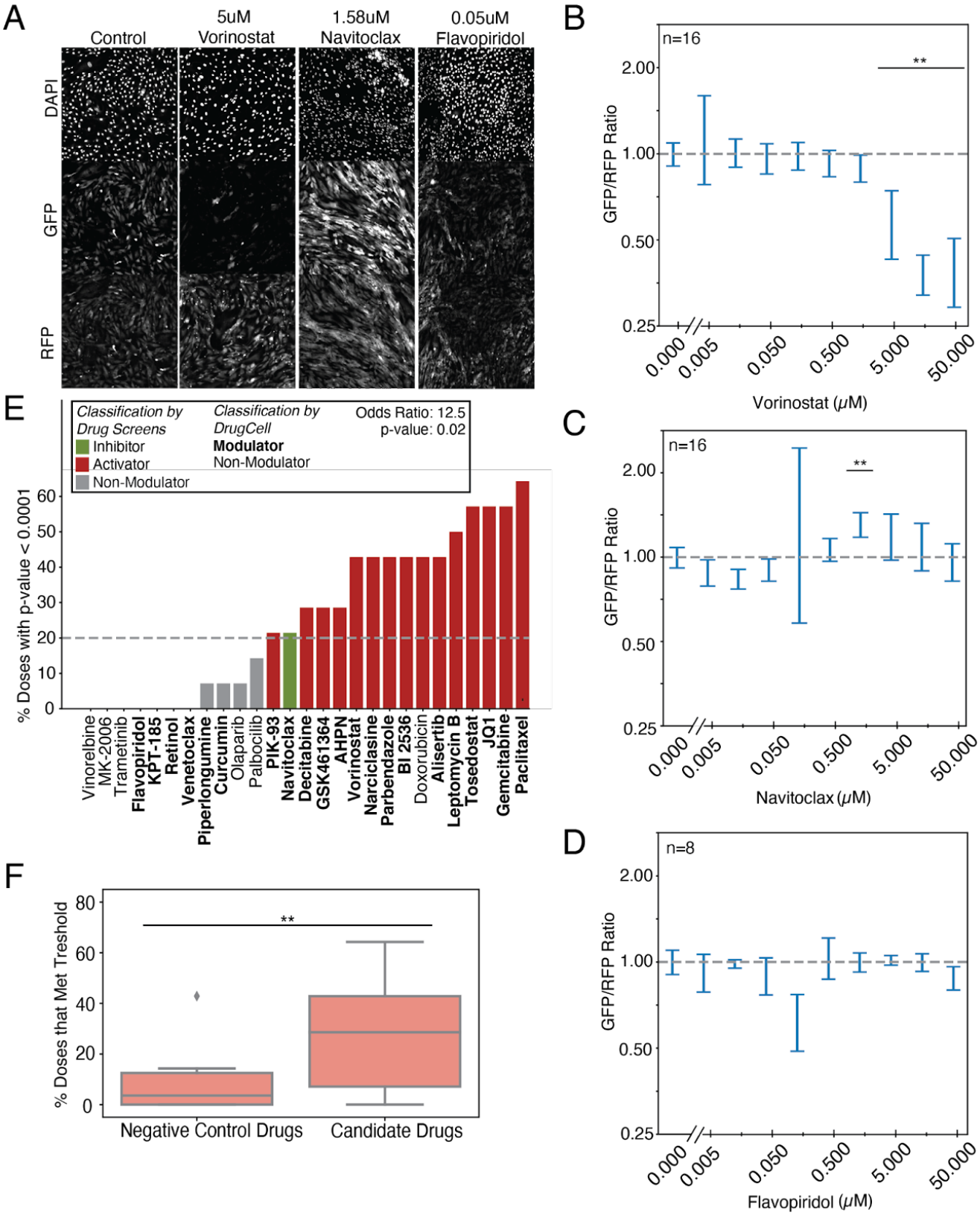
A
Control
5uM Vorinostat
1.58uM Navitoclax
0.05uM Flavopiridol
DAPI
GFP
RFP
B
n=16
**
GFP/RFP Ratio
2.00
1.00
0.50
0.25
0.000
0.005
0.050
0.500
5.000
50.000
Vorinostat (μM)
C
n=16
**
GFP/RFP Ratio
Navitoclax (μM)
D
n=8
GFP/RFP Ratio
Flavopiridol (μM)
E
Classification by Drug Screens
Inhibitor
Activator
Non-Modulator
Classification by DrugCell
Modulator
Non-Modulator
Odds Ratio: 12.5
p-value: 0.02
% Doses with p-value < 0.0001
Vinorelbine
MK-2006
Trametinib
Flavopiridol
KPT-185
Retinol
Venetoclax
Piperlongumine
Curcumin
Olaparib
Palbociclib
PIK-93
Navitoclax
Decitabine
GSK461364
AHPN
Vorinostat
Narciclasine
Parbendazole
BI 2536
Doxorubicin
Alisertib
Leptomycin B
Tosedostat
JQ1
Gemcitabine
Paclitaxel
F
% Doses that Met Treshold
**
Negative Control Drugs
Candidate Drugs

Examination of Potential Synergies between Autophagy Activators and Chloroquine

Finally, we tested eight out of the fourteen autophagy activators found above for synergistic effects with chloroquine. RPE1-pMRX single clones were subjected to a combined treatment of each activator and chloroquine. When two drugs are in synergy, the combined effect of the drugs on cell viability is greater than the sum of the effects of the two drugs alone. To determine whether two drugs are synergistic we looked at the effect of both drugs on cell viability compared to that of each drug alone and calculated the Bliss synergy score for each combination. A Bliss synergy score greater than 10 suggests that the drug combination is synergistic. The combined treatment of tosedostat and chloroquine caused significantly more cell death than did either of the drugs alone ($p < 0.05$; Figures 4A,B). This specific drug pair had a Bliss synergy score of 12.95, indicating that at those doses, tosedostat and chloroquine are synergistic. Four out of the eight drugs tested (JQ1, tosedostat, leptomycin B, and vorinostat) had Bliss synergy > 10 in combination with chloroquine (Figure S4,5). Three of these (tosedostat, leptomycin B, and vorinostat) led to greater than 20% inhibition over the maximum achieved by the single agents alone (Figure S4). The highest Bliss synergy scores were for vorinostat and chloroquine (Figure 4C). At the specific dose pairs that we found a high Bliss synergy score, we observed an increase in GFP/RFP ratios, indicating that chloroquine-mediated inhibition of autophagy prevents vorinostat-mediated activation of proliferation mechanisms through the activation of autophagy. Such results suggest that the inhibition of autophagy when activated by a cancer drug can help prevent chemoresistance and induce cytotoxic effects and cell death.

Figure 4. Combination of Predicted Drugs and Chloroquine

(A) Effect of single and combined treatment of tosedostat with chloroquine on cell inhibition at the indicated doses and the bliss synergy score of drug combination; combination treatment compared to control, tosedostat alone, and chloroquine alone had p-values<0.05 (indicated with **)

(B) Microscopy images (4x) under DAPI channel of RPE1-pMRX under no drug, 10.48uM tosedostat, 2.18uM chloroquine, and tosedostat and chloroquine combinated

(C) Bliss synergy scores of the combination treatment of vorinostat and chloroquine at indicated doses

(D) Effect of vorinostat and chloroquine on GFP/RFP ratios at indicated doses

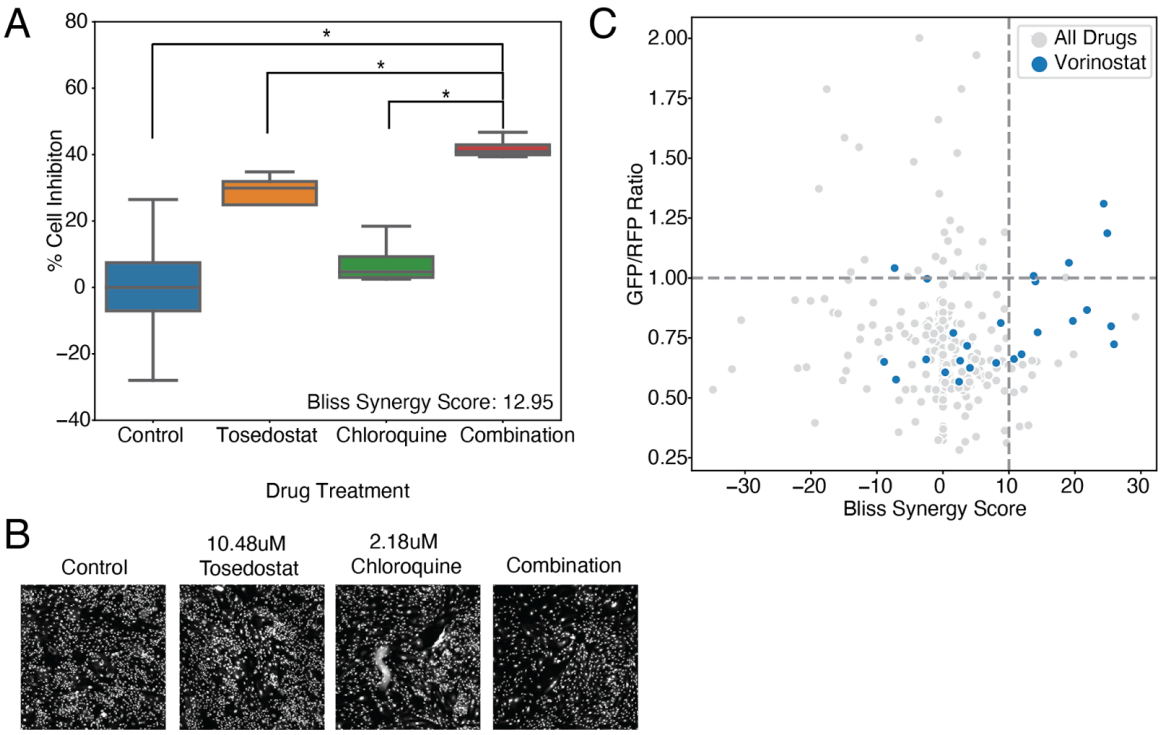

Discussion

Cancer exploits autophagy to continue proliferating by inducing chemoresistance mechanisms. We found 14 chemotherapies that were predicted to modulate autophagy by DrugCell to activate autophagy, whereas only one of them was found to be an autophagy inhibitor. One reason as to why DrugCell has a bias towards autophagy activators versus inhibitors could be due to the fact that when a drug causes a certain level of stress on the drug, autophagy is activated in response, rather than inhibited. As we see that all three of the PLK1 inhibitors, both of the replicative stress inducers, and both of the microtubular modifiers, disruption of different pathways causes an overall stress on the cell, leading to the activation of autophagy.

Doxorubicin was the only drug that DrugCell predicted to not modulate autophagy, however, our drug screens showed that it activates autophagy. A potential reason for why doxorubicin was predicted as a non-modulator versus a modulator could be because of the how DrugCell is trained. DrugCell screens various cancer cell lines, specifically the genotypes, along

with drug structures to predict a cell's response to a drug. For the 21 candidate drugs that were predicted to modulate autophagy, there could have been a strong genetic background that showed mutations in autophagy genes are associated with the predicted autophagy modulators. For doxorubicin, it is possible that there is not as strong of a genetic background that caused DrugCell to believe it was not an autophagy modulator.

All the drug screens performed were using wild-type cell lines, meaning that the cells under no treatment, are not under any stress. It is only when drug is added, the cells experience stress. However, this is the opposite with cancer cells. Cancer cells experience some sort of stress even when not treated with a drug. Therefore, these drug screens could be repeated in a cancer cell line to see whether the drug combinations deemed synergistic remain synergistic in a cancer context.

The most synergistic drug combination was found to be vorinostat and chloroquine. To determine the molecular drives of such phenotype, a chemogenetic screen could be performed where we target known autophagy genes using CRISPR, subject the cells to combination treatment of vorinostat and chloroquine, and analyze the effects of such alterations.

This thesis, in full, is a reprint of the material as it will appear in A Neural Network Model of Cancer Identifies Chemotherapies Synergistic with Autophagy Inhibition. Aradhyula, Likitha Y.; Silva, Erica; Fong, Samson H.; Rajaee, Lily; Ideker, Trey. The thesis author was the primary investigator and author of this paper.

Methods

Selection of Candidate Drug List via DrugCell

To select candidate drugs that are predicted to modulate autophagy, we first identified the five core GO-terms that were associated with the autophagy pathway. We also used the REACTOME pathway database to identify genes that are known to be related to autophagy. With the genes that overlapped the REACTOME pathway database and the genes in DrugCell, we identified ten additional GO-terms that are highly enriched for the genes in the autophagy pathway. Then, we looked for drugs that had an RLIPP score greater than 1 for the autophagy terms, core and associated. We then narrowed down the list to 21 drugs using literature review.

Gibson Cloning of Neomycin Selection Marker into the Fluorescent Autophagy Reporter

To measure autophagy activity in future screens, we used a fluorescent autophagy reporter called pMRX-IP-GFP-LC3-RFP-LC3ΔG (pMRX-Puro, Addgene#84572). For pMRX-Puro to be compatible with future screening protocol, we replaced the puromycin resistance cassette (PuroR) with a neomycin resistance cassette (NeoR). Primers, listed in Table 1, were used to amplify the Pmrx backbone without the PuroR gene and the NeoR from Paavs1-Ndi-CRISPRi Gen 2 (Addgene #73498). The Pmrx backbone and NeoR gene were amplified by polymerase chain reaction (PCR, KAPA HiFi 2x MasterMix #7958927001). The PCR products were then purified to remove impurities and primer dimers through column purification (NEB, #T1030S). The NeoR insert was cloned into the Pmrx-backbone using Gibson cloning according to manufacturer directions, resulting in the neomycin-resistant Pmrx reporter (Pmrx) (NEB, #E2611S). The products were again column-purified and transformed into chemically-competent E. coli (Thermofisher, #C737303). The transformation mix was then plated onto ampicillin selection plates and the resulting colonies were verified by colony PCR (Thermofisher, #F160S)

using the primers listed in Table 1. The colonies were inoculated and resulting cultures were mini-prepped to extract the Pmrx (ZymoPure Plasmid MiniPrepKit #D4211). The sequence was confirmed by Sanger Sequencing using the primers IRES-F, Pmrx-selection-F, and Pmrx-selection-R, which sequences can be found in Table 2.

Generation of Stable Single Clone Cell Lines that Measure Autophagy Activity

We used transduction to generate cell lines that express the Pmrx reporter along with a Cas9 plasmid. PlatA virus (#RV-102) were transfected (ThermoFisher, #L3000001) with Pmrx along with Lipofectamine according to manufacturer instructions to produce Pmrx retrovirus. Cos7 cells were transfected with pLenti-Cas9-T2A-BFP (Addgene #78547), Pcmv-Dr8.2 dvpr (Addgene #8455) and Pmd2.G (Addgene #12259) with Lipofectamine to produce Cas9 lentivirus. Viral supernatant from both transfections were separately collected two and four days post transfection and was concentrated (Amicon, #UFC910024). Htert-immortalized human retinal pigment epithelial cells (RPE1) were maintained in DMEM/F12 + 10% FBS. On day 1, RPE1 were co-infected with the Pmrx retrovirus and Cas9 lentivirus. 24 hours later, the infected RPE1 cells went under neomycin selection at 400ug/Ml and blasticidin selection at 5ug/Ml. After selection and expansion, the polyclonal RPE1 cell lines that express Pmrx and Cas9 were then diluted and plated to generate single clones. After two weeks, the single clonal RPE1 cell lines that express Pmrx and Cas9 (RPE1-Pmrx) were then isolated using colony rings and were under a maintenance dose of 40ug/Ml geneticin and 0.5ug/Ml blasticidin.

Validation of Fluorescent Autophagy Reporter in RPE1-Pmrx

To ensure the Pmrx reporter in the single clone cell lines accurately measures autophagy activity, the cell lines were plated onto coverslips in 6-well plates with a density of 1.0x10 cells/well on day 1. On day two, the cells were then washed twice with PBS and subjected to

different conditions: grown in complete media (DMEM/F12 + 10% FBS), grown in serum starvation media using DMEM –Met/Cys serum-free media, or grown in serum starvation media along with 5Um chloroquine. After 24 hours of treatment, the cells were then washed with PBS and fixed with cold 4% PFA in PBS for 10 minutes at room temperature, followed by another three washes of PBS. They were then stained with 5ug/Ml Hoechst for fifteen minutes and washed again with PBS three times. The stained coverslips were mounted onto microscope slides with Fluoromount G (#00-4958-02). The coverslips mounted onto slides were imaged using the Keyence (BZ-X810; 20x objective; CY3/R, DAPI, EGFP filters) and the images were then analyzed with ImageJ to measure GFP and RFP intenstities.

Cas9 Cutting Efficiency Assay in RPE1-Pmrx

To ensure the single clone RPE1-Pmrx have high Cas9 cutting efficiency, the RPE1-Pmrx were plated into 6-well plates with a density of 1.0x10 cells/well on day 1. On day two, the cells were infected with Pxpr_011 (Addgene #59702). After 24 hours later, the cells were selected with 15ug/Ml puromycin. The cells were lifted on Day 8 and Day 15 their GFP fluorescence was measured using flow cytometry.

Single Drug Titer of the Predicted Drugs

To identify which chemotherapies modulate autophagy, two of the functionally validated RPE1-Pmrx single clones were separately plated into 384 well plates (Corning, #3764) with a density of 1.5x10cells/well on day 1. The doses of the drugs tested ranged from 0Um to 50Um and were prepared using serial dilutions. The prepared doses of drugs were stored in the -80°C freezer. On day 2, the prepared doses of drugs were thawed at room temperature and were added to the respective wells in the 384 well plate. After 48 hours of treatment, the cell plates were washed with PBS twice, fixed and stained with 4% PFA in PBS with 10ug/Ml Hoechst for

5 minutes. The cell plate was washed again with PBS three times. The fixation and staining was done using the Tecan () with a programmed protocol. Post fixation and staining, the cell plates were imaged using the Keyence (BZ-X810) with the 10x objective and CY3/R, DAPI, EGFP filters to measure for autophagy and 4x objective with the DAPI filter to measure cell viability. Python was used to analyze the fluorescence images. To select which of the candidate drugs modulated autophagy, we calculated the GFP/RFP of RPE1-Pmrx treated by each dose of each drug and normalized each ratio to the ratio of RPE1-Pmrx that received no drug. These ratios were tested for statistical significance using t-tests and corrected the p-value using the Bonferroni method. The doses that were deemed significant had a corrected p-value less than 0.001. Drugs that had at least 20% of doses with a significant GFP/RFP ratio were considered as autophagy modulators. The negative control drugs that were tested were subjected to the same thresholds.

Drug Combination Experiments between Predicted Drugs and Chloroquine

The drugs that were found to actually modulate autophagy were tested in combination with chloroquine to determine which of those drugs are synergistic with chloroquine. The RPE1-Pmrx single clones were plated into 384 well plates (Corning, #3764) with a density of 1.5x10cells/well on day 1. The doses of the drugs in question and chloroquine ranged from 0Um to 50Um were prepared using serial dilutions. The prepared doses of drugs were stored in the -80°C freezer. On day 2, the prepared doses of drugs were thawed at room temperature and were added to the respective wells in the 384 well plate. After 48 hours of treatment, the cell plates were washed with PBS twice, fixed and stained with 4% PFA in PBS with 10ug/Ml Hoechst for 5 minutes. The cell plate was washed again with PBS three times. The fixation and staining was done using the Tecan () with a programmed protocol. Post fixation and staining, the cell plates were imaged using the Keyence (BZ-X810) with 4x objective with just the DAPI filter to measure cell viability along with the 10x objective and CY3/R, DAPI, EGFP filters to measure for

autophagy. Python was used to analyze the images to extract cell count and GFP/RFP ratios. We utilized Synergy Finder[2] to calculate Bliss synergy scores for each drug combination. To determine which drug pairs were truly synergistic, we first looked for drug combinations that had certain dose pairs with a Bliss synergy score greater than 25. Out of those drug pairs, we looked for dose pairs that had 20% more inhibition than the max inhibition of the single drugs.

Table 1. PCR Amplification Primers

Primer Sequence	Purpose of Primers
5'- gttcttctgacgcccgccccacgacccg – 3'	Amplified the backbone of the Pmrx-Puro
5'- ccgatcccatggttgtggccatattatcatcgtgtttttcaaaggaaaaccacgtccc – 3'	
5'- ggccacaaccatgggatcggccattgaac-3'	Amplified the NeoR gene from the Paavs1-Ndi-CRISPRi Gen 2
5'-ggggcgggcgtcagaagaactcgtcaagaag-3'	

Table 2. Sequencing Primers

Primer Sequence	Name of Primer
5'-tggctctcctcaagcgtatt-3'	IRES-F
5'-tggacgaagagcatcaggggctcgc-3'	Pmrx-selection-F
5'-atggggtcgtgcgctcctttc-3'	Pmrx-selection-R

Appendix

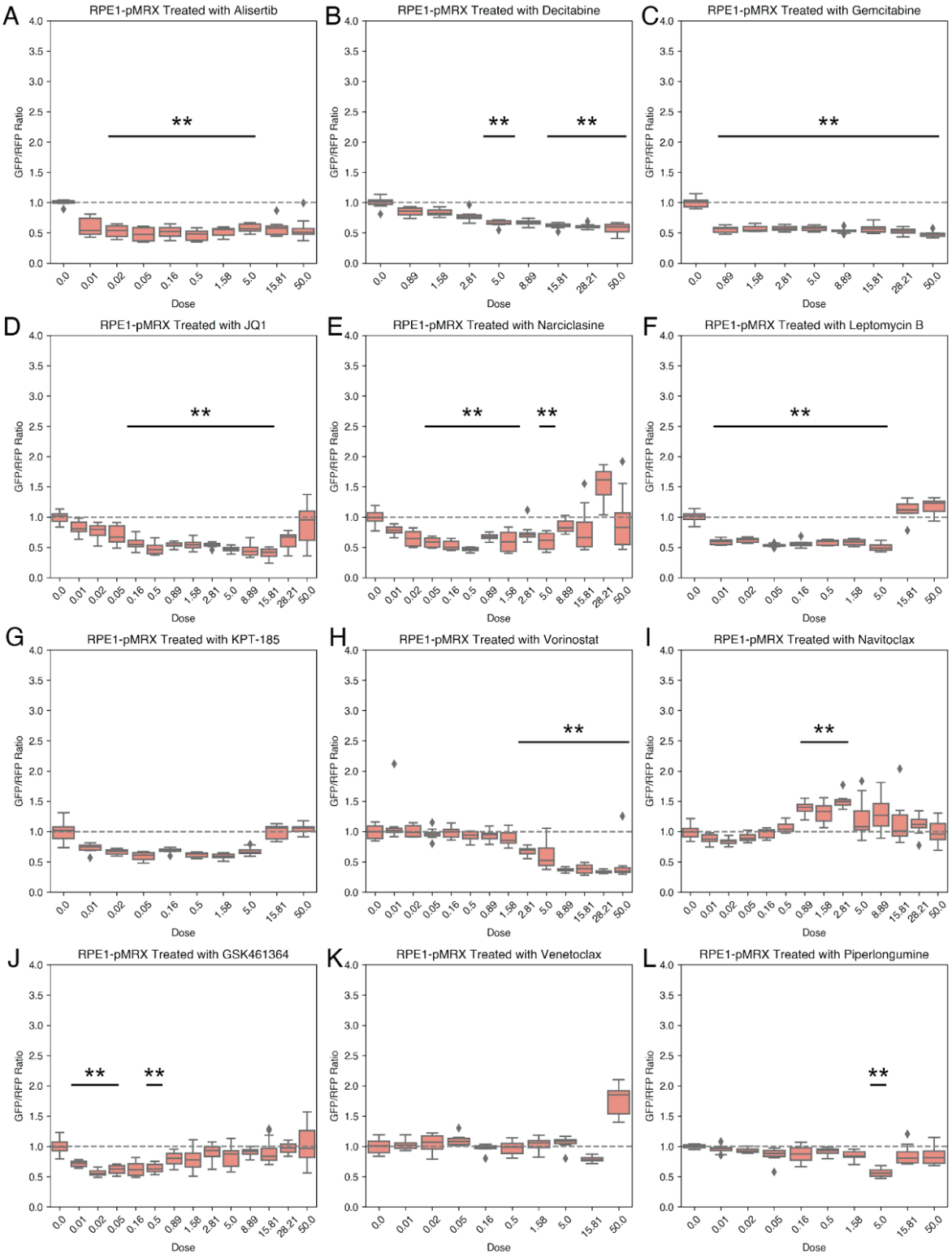

Figure S1. GFP/RFP Ratios of RPE1-pMRX Treated with Candidate Drug List

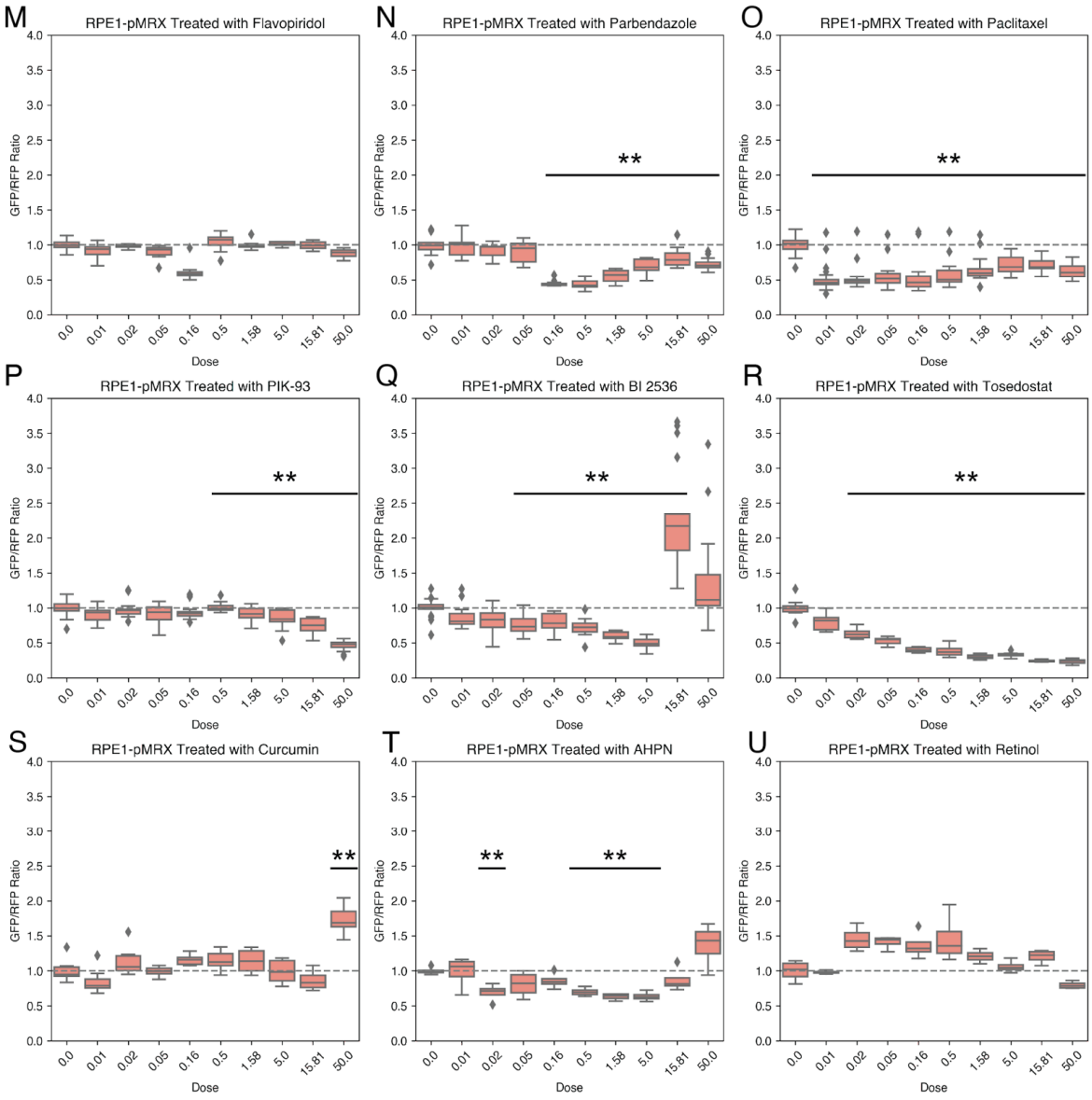

Figure S1. GFP/RFP Ratios of RPE1-pMRX Treated with Candidate Drug List (Continued)

(A-U) Boxplots that depict the GFP/RFP ratios of RPE1-pMRX treated a range of doses of the drug indicated; statistical significance depicted by asterisks (**)

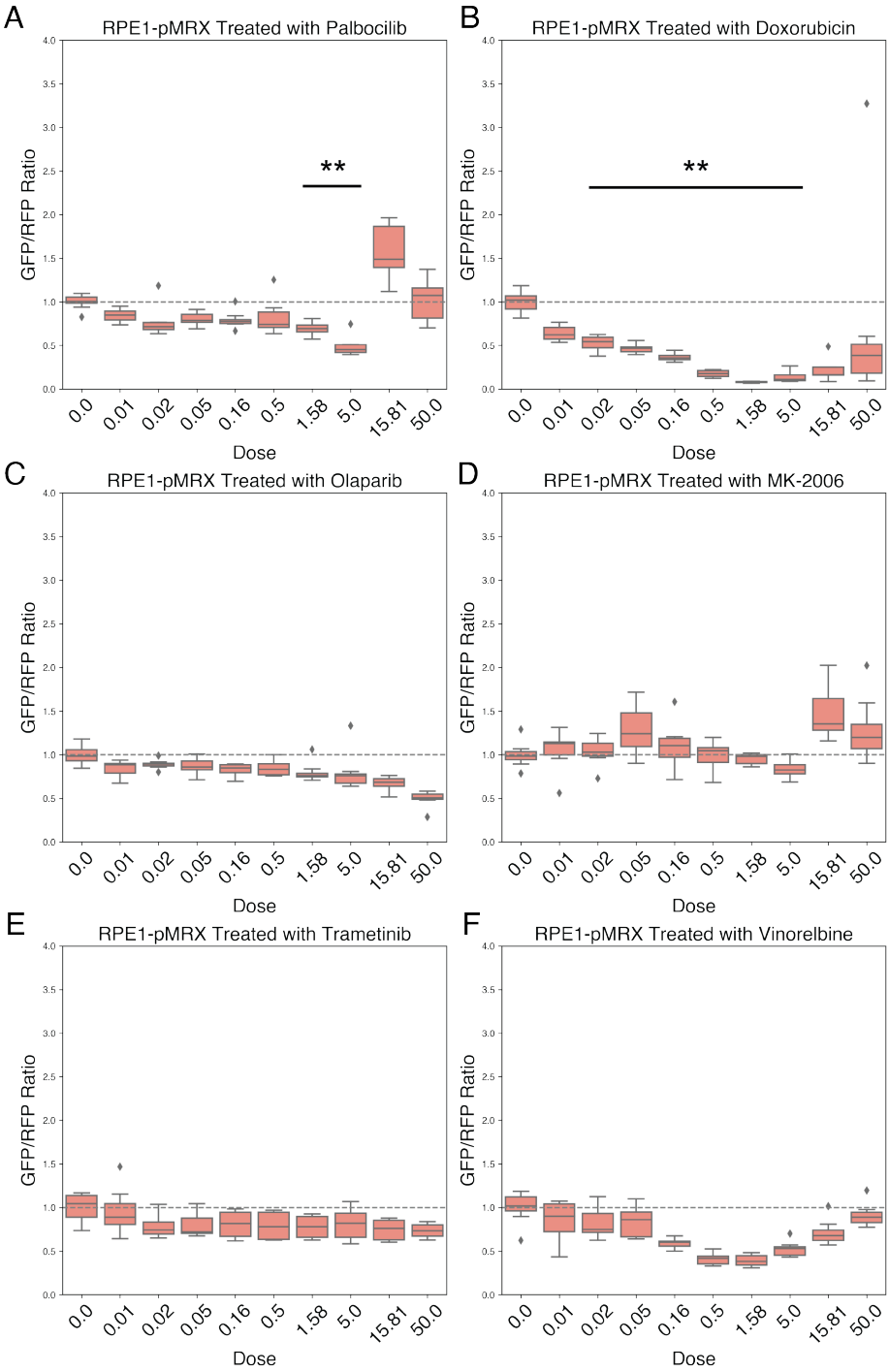

Figure S2. GFP/RFP Ratios of RPE1-pMRX Treated with Negative Control Drugs

(A-F) Boxplots that depict the GFP/RFP ratios of RPE1-pMRX treated a range of doses of the drug indicated; statistical significance depicted by asterisks (**)

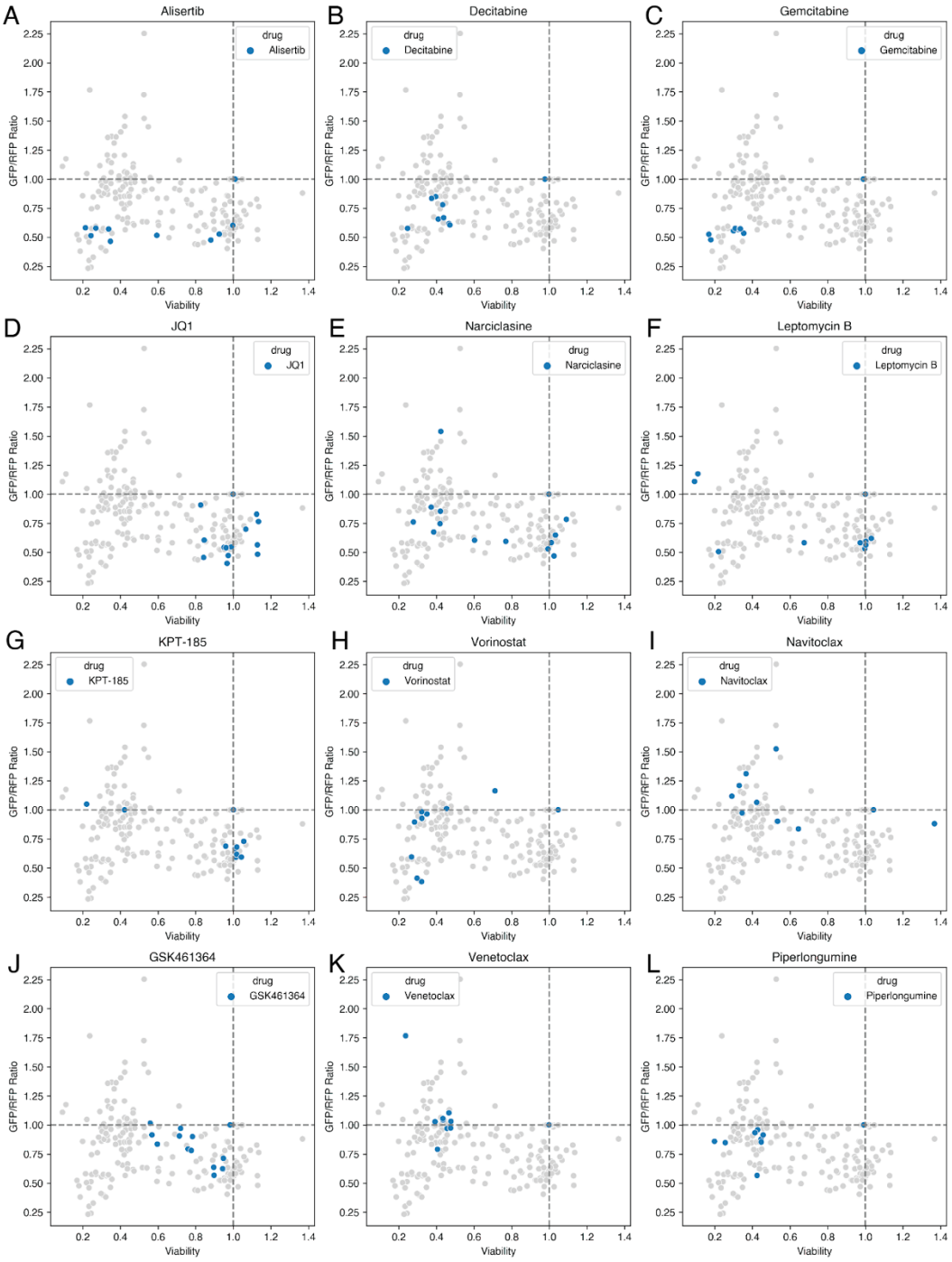

Figure S3. Effect of Candidate Drug List of Candidate Drug List on Viability and GFP/RFP Ratios

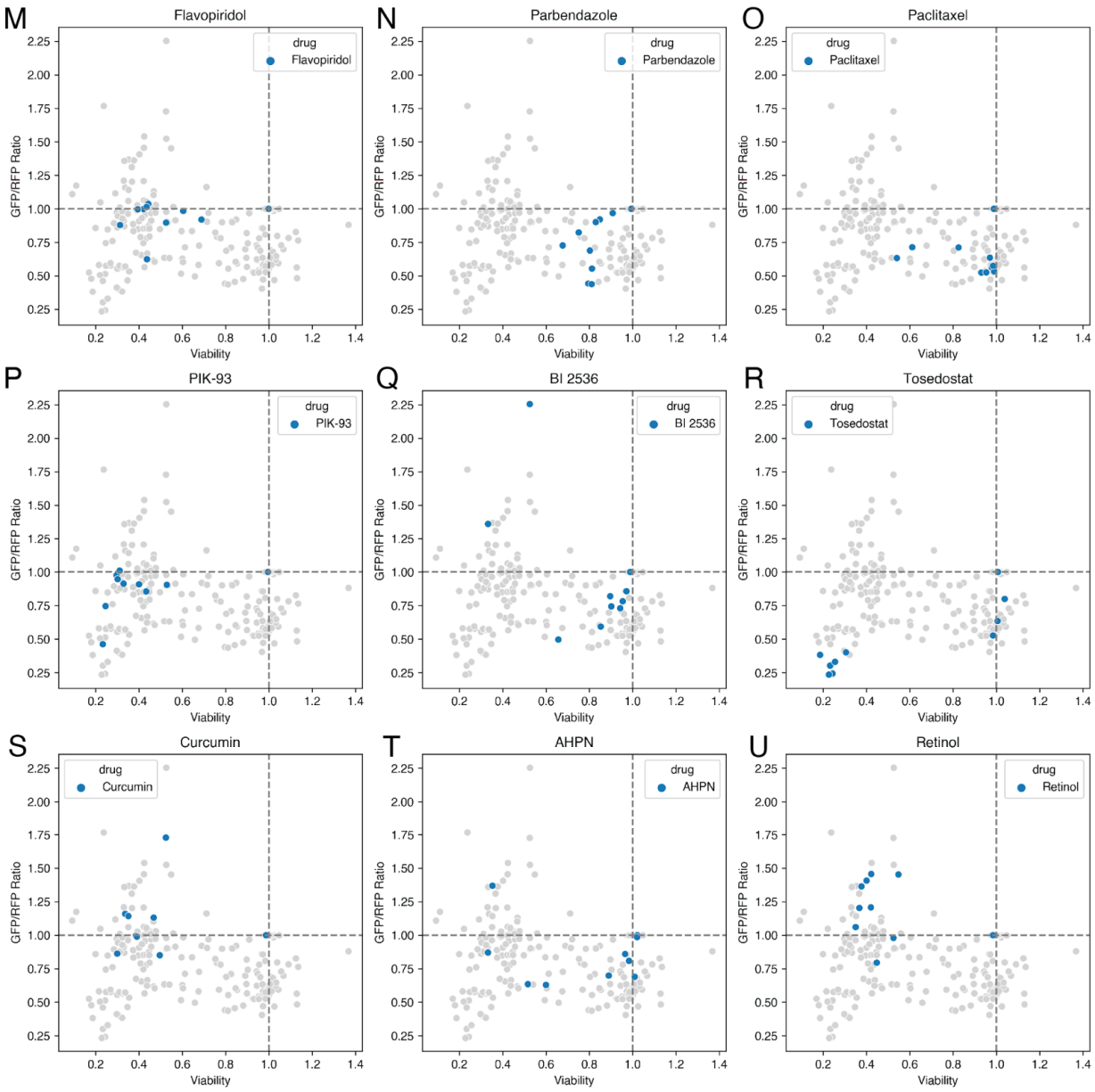

Figure S3. Effect of Candidate Drug List of Candidate Drug List on Viability and GFP/RFP Ratios (Continued)

(A-U) Scatterplots that depict the effect of the indicated drug (blue) on the viability and GFP/RFP ratios of RPE1-pMRX compared to the effect of all the candidate drugs (gray)

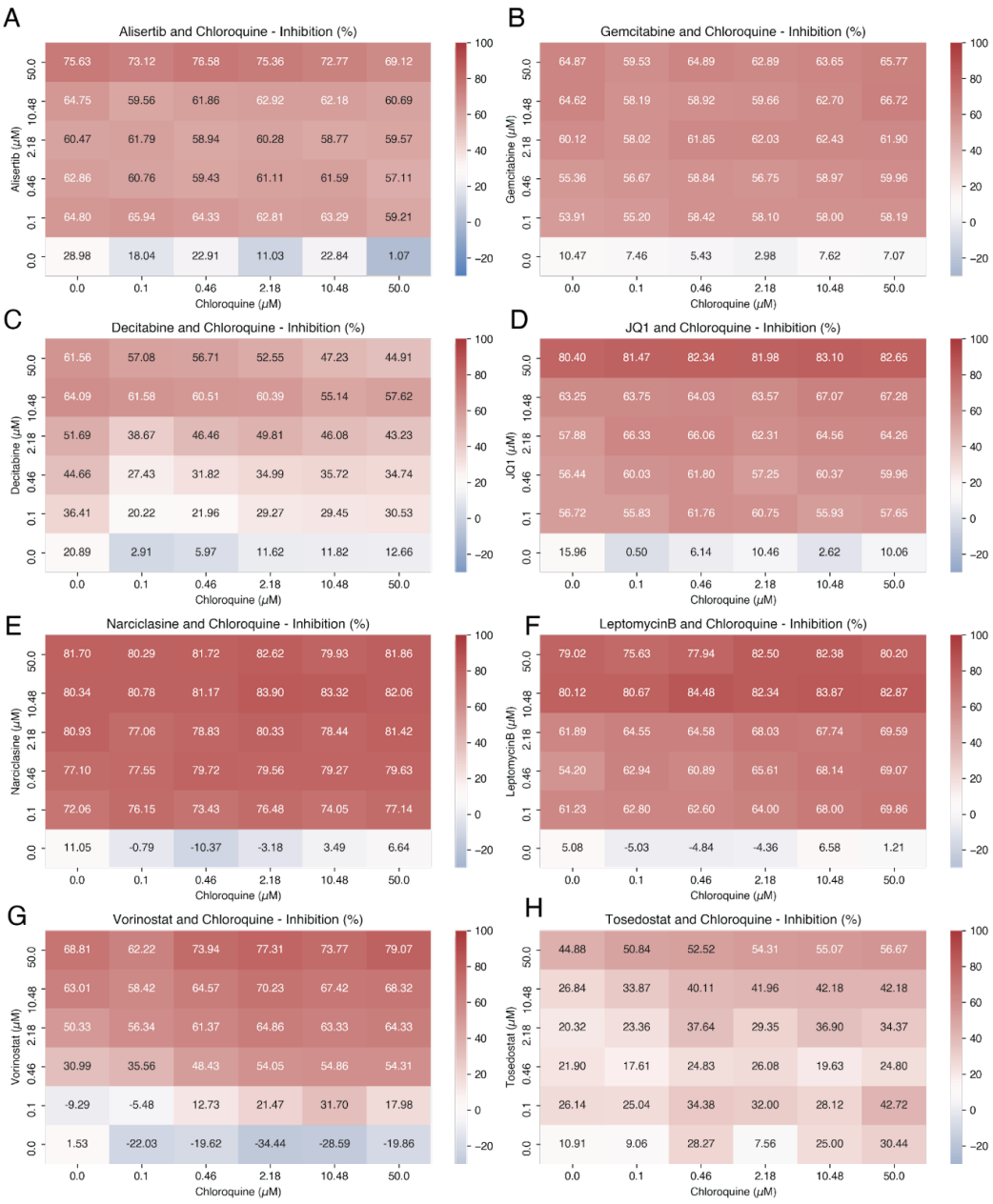

Figure S4. Effect of Drug Combinations of Cell Inhibition

(A-H) Effect of the combined treatment of the indicated drug and chloroquine on the cell inhibition of RPE1-pMRX at the indicated doses

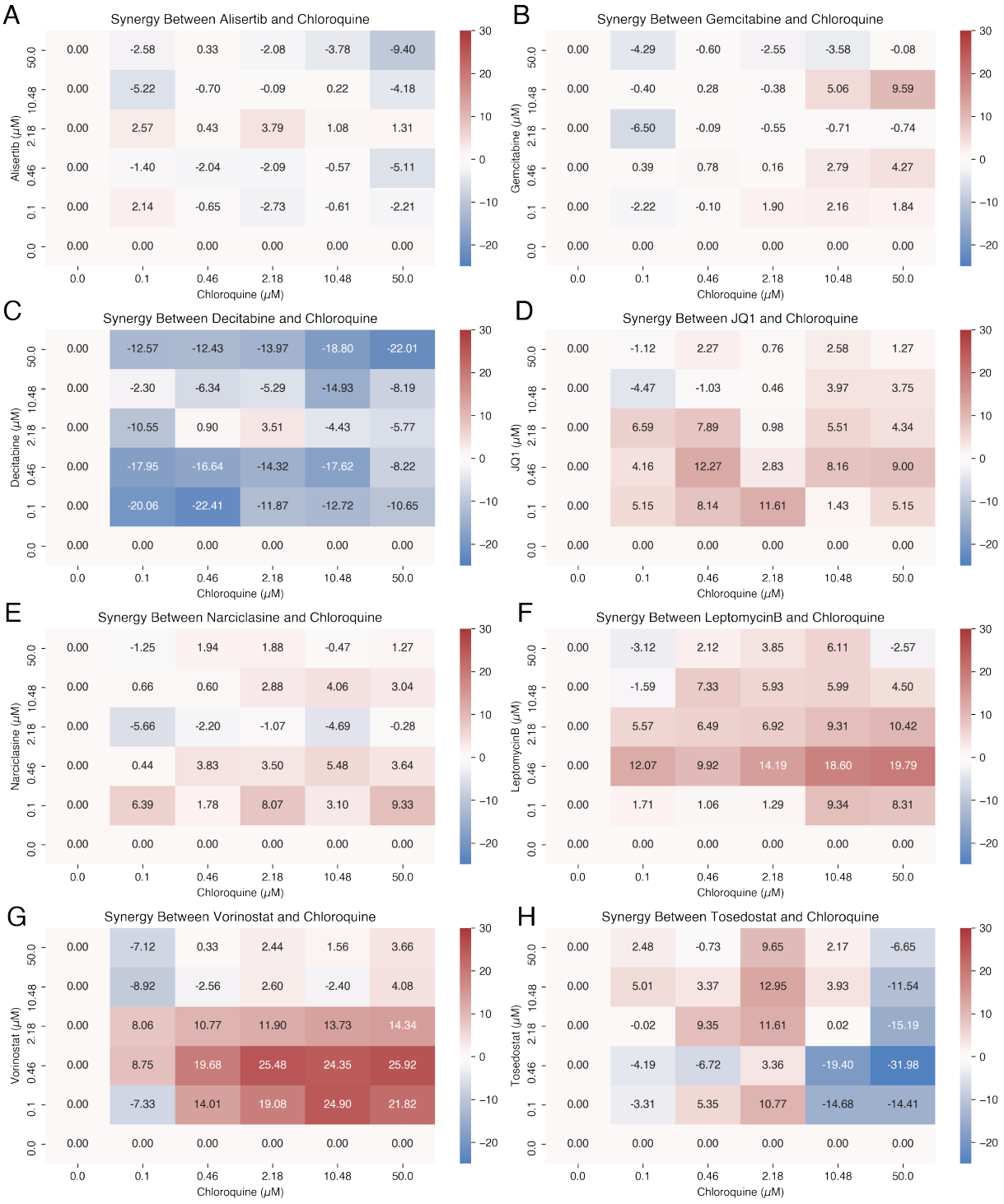

Figure S5. Bliss Synergy Scores of Drug Combinations

(A-H) Bliss synergy scores of the combined treatment of the indicated drug and chloroquine on RPE1-pMRX

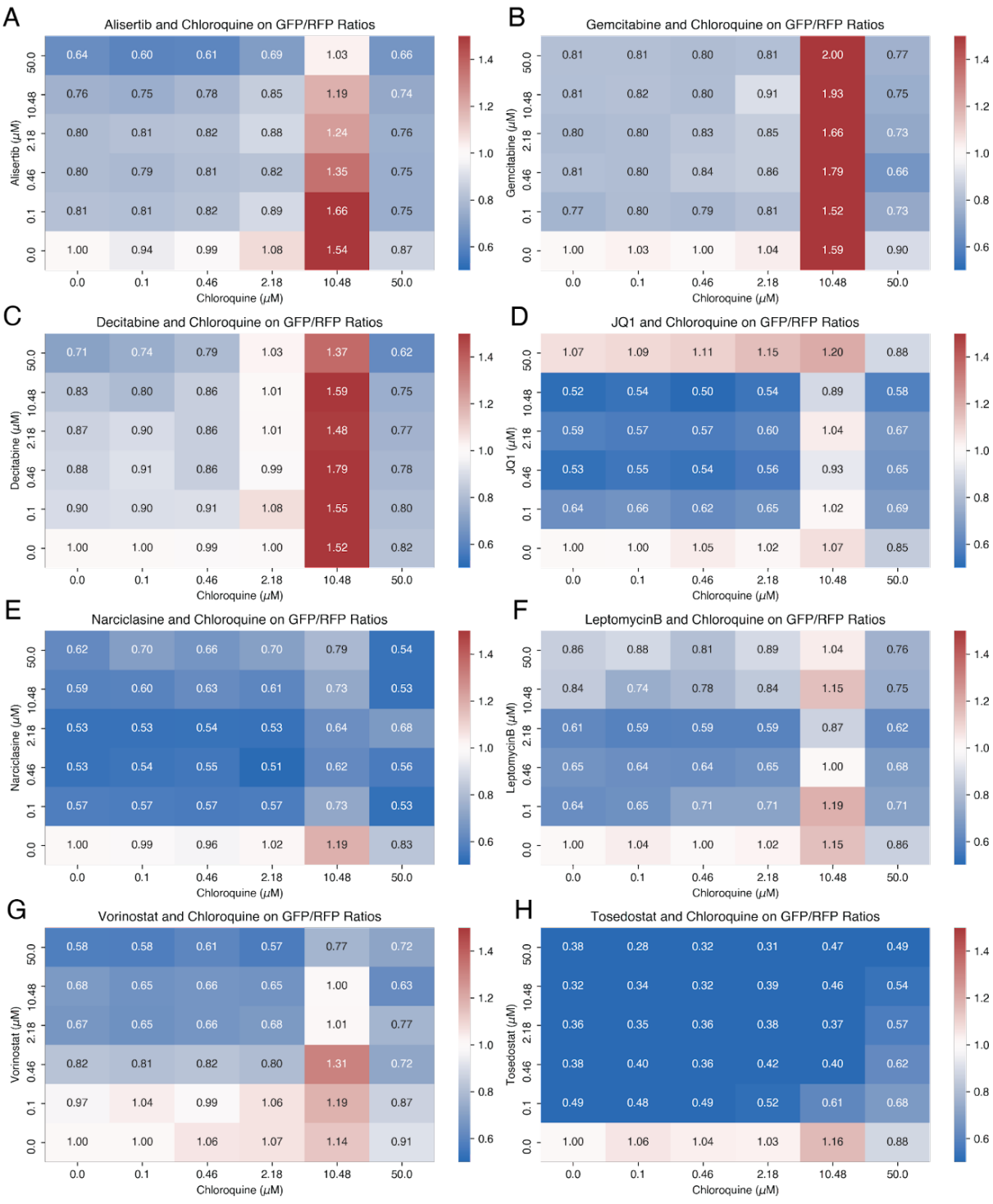

Figure S6. Figure S4. Effect of Drug Combinations of Cell Inhibition

(A-H) GFP/RFP ratios of RPE1-pMRX that were co-treated with the indicated drug and chloroquine

References

1. Balgi, A. D., Fonseca, B. D., Donohue, E., Tsang, T. C. F., Lajoie, P., Proud, C. G., Nabi, I. R., & Roberge, M. (2009). Screen for chemical modulators of autophagy reveals novel therapeutic inhibitors of mTORC1 signaling. *PloS One*, *4*(9), e7124. https://doi.org/10.1371/journal.pone.0007124
2. Chauhan, S., Ahmed, Z., Bradfute, S. B., Arko-Mensah, J., Mandell, M. A., Won Choi, S., Kimura, T., Blanchet, F., Waller, A., Mudd, M. H., Jiang, S., Sklar, L., Timmins, G. S., Maphis, N., Bhaskar, K., Piguet, V., & Deretic, V. (2015). Pharmaceutical screen identifies novel target processes for activation of autophagy with a broad translational potential. *Nature Communications*, *6*, 8620. https://doi.org/10.1038/ncomms9620
3. Duan, L., Motchoulski, N., Danzer, B., Davidovich, I., Shariat-Madar, Z., & Levenson, V. V. (2011). Prolylcarboxypeptidase Regulates Proliferation, Autophagy, and Resistance to 4-Hydroxytamoxifen-induced Cytotoxicity in Estrogen Receptor-positive Breast Cancer Cells*. *The Journal of Biological Chemistry*, *286*(4), 2864–2876. https://doi.org/10.1074/jbc.M110.143271
4. Hundeshagen, P., Hamacher-Brady, A., Eils, R., & Brady, N. R. (2011). Concurrent detection of autolysosome formation and lysosomal degradation by flow cytometry in a high-content screen for inducers of autophagy. *BMC Biology*, *9*, 38. https://doi.org/10.1186/1741-7007-9-38
5. Ianevski, A., Giri, A. K., & Aittokallio, T. (2020). SynergyFinder 2.0: visual analytics of multi-drug combination synergies. *Nucleic Acids Research*, *48*(W1), W488–W493. https://doi.org/10.1093/nar/gkaa216
6. Kaizuka, T., Morishita, H., Hama, Y., Tsukamoto, S., Matsui, T., Toyota, Y., Kodama, A., Ishihara, T., Mizushima, T., & Mizushima, N. (2016). An Autophagic Flux Probe that

Releases an Internal Control. *Molecular Cell*, *64*(4), 835–849. https://doi.org/10.1016/j.molcel.2016.09.037

7. Kuenzi, B. M., Park, J., Fong, S. H., Sanchez, K. S., Lee, J., Kreisberg, J. F., Ma, J., & Ideker, T. (2020). Predicting Drug Response and Synergy Using a Deep Learning Model of Human Cancer Cells. *Cancer Cell*, *38*(5), 672–684.e6. https://doi.org/10.1016/j.ccell.2020.09.014
8. Levine, B., & Kroemer, G. (2008). Autophagy in the pathogenesis of disease. *Cell*, *132*(1), 27–42. https://doi.org/10.1016/j.cell.2007.12.018
9. Levine, B., & Kroemer, G. (2019). Biological Functions of Autophagy Genes: A Disease Perspective. *Cell*, *176*(1-2), 11–42. https://doi.org/10.1016/j.cell.2018.09.048
10. Mizushima, N. (2018). A brief history of autophagy from cell biology to physiology and disease. *Nature Cell Biology*, *20*(5), 521–527. https://doi.org/10.1038/s41556-018-0092-5
11. Paillas, S., Causse, A., Marzi, L., de Medina, P., Poirot, M., Denis, V., Vezzio-Vie, N., Espert, L., Arzouk, H., Coquelle, A., Martineau, P., Del Rio, M., Pattingre, S., & Gongora, C. (2012). MAPK14/p38α confers irinotecan resistance to TP53-defective cells by inducing survival autophagy. *Autophagy*, *8*(7), 1098–1112. https://doi.org/10.4161/auto.20268
12. Sui, X., Chen, R., Wang, Z., Huang, Z., Kong, N., Zhang, M., Han, W., Lou, F., Yang, J., Zhang, Q., Wang, X., He, C., & Pan, H. (2013). Autophagy and chemotherapy resistance: a promising therapeutic target for cancer treatment. *Cell Death & Disease*, *4*, e838. https://doi.org/10.1038/cddis.2013.350
13. Zhang, L., Yu, J., Pan, H., Hu, P., Hao, Y., Cai, W., Zhu, H., Yu, A. D., Xie, X., Ma, D., & Yuan, J. (2007). Small molecule regulators of autophagy identified by an image-based

high-throughput screen. *Proceedings of the National Academy of Sciences of the United States of America*, *104*(48), 19023–19028. https://doi.org/10.1073/pnas.0709695104